Chapter 14

Modeling and Experimental Investigation of Light Intensity and Initiator Effects on Solvent-Free Photopolymerizations

Michael D. Goodner and Christopher N. Bowman[1]

Department of Chemical Engineering, Campus Box 424, University of Colorado, Boulder, CO 80309–0424

The free radical photopolymerization of 2-hydroxyethyl methacrylate (HEMA) initiated by 2,2-dimethoxy-2-phenylacetophenone (DMPA) is studied using kinetic model predictions and experiments. Both homogeneous and spatially varying kinetic models are developed from species balances on reacting species in the polymerization system. The focus of this investigation is the effect of incident light intensity and photoinitiator concentration on the polymerization kinetics. In optically thin samples, the polymerization rate profiles are shown to have the classical square root dependence on both light intensity and initiator concentration in the absence of primary radical termination. Homogeneous model predictions incorporating primary radical termination show reduction and, at higher primary radical concentrations, elimination of autoacceleration and a reduction in the final conversion. These features can be attributed to the quenching effect that the primary radicals have on the macroradical population. The effect of sample thickness is investigated using a kinetic model incorporating spatial variations in one dimension. Optically thick samples show marked decreases in rate and conversion at the bottom of thick films, while use of photobleaching initiators can partially mitigate these effects.

Bulk polymerization of vinyl monomers provides a convenient route for production of polymeric materials used in a wide variety of applications. Materials formed via free-radical polymerizations include lithographic plates, photoresists, protective coatings, adhesives, and biomedical devices, such as controlled-release matrices and dental restorations (*1-4*). Because the monomers used in these processes are liquids of intermediate viscosity, no solvent is needed to carry out the polymerization in the liquid phase. In addition to any environmental benefits, the lack of a solvent reduces complications resulting from spurious and unwanted chain transfer reactions, along with providing greater rates of polymerization at low conversions.

Unfortunately, the kinetics of solvent-free polymerizations are greatly complicated at higher conversions in both the formation of linear polymers and the production of crosslinked systems. As viscosity and vitrification effects increase, autoacceleration begins, greatly increasing the rate of polymerization (*1,3*). For these highly exothermic polymerization reactions, increased rate translates into increased heat production. Without a solvent to dilute the system and remove the excess heat of

[1]Corresponding author: telephone: 303–492–3247; fax: 303–492–4341; e-mail: bowman@colorado.edu.

Long and Hunt; Solvent-Free Polymerizations and Processes
ACS Symposium Series; American Chemical Society: Washington, DC, 1999.

polymerization, charring and volatilization can potentially ruin the desired product. At even greater conversions, vitrification leads to autodeceleration and incomplete functional group conversion despite continued initiator presence and exposure to light. Unincorporated monomer can leach from the polymer system, leading to toxicity effects, especially in biomedical polymers. In crosslinked systems, unreacted pendent double bonds can react in the post-cure period, leading to brittleness and decreased permeability.

One method used to minimize viscosity and vitrification effects is to carry out the polymerizations at high initiation and polymerization rates (*5*). Due to the incorporation of many monomer units into each polymer molecule, volume shrinkage occurs upon polymerization. At high polymerization rates, conversion of monomer to polymer occurs at a much faster rate than the volume shrinkage. As a result, reacting molecules are afforded extra mobility, and the polymerizing system can reach much greater conversions than could be achieved while maintaining equilibrium volume shrinkage (*1,5-7*).

To reach higher polymerization rates, the population of growing polymer chains must be increased throughout the polymerization. The easiest route to achieve this goal is to increase the rate of initiation. However, in photopolymerizations, several effects pose difficulties when trying to reach higher initiation rates. Increasing the photoinitiator concentration in a monomer solution has the undesirable consequence of reducing light penetration. In a protective coating, this effect can result in a hard, tack-free surface that will not adhere to a delicate substrate because of the reduced polymerization at the bottom of the film. Increased photoinitiator content can also result in pronounced yellowing of the product that is associated with excess photoinitiator not incorporated into the polymer network. Increasing light intensity to reach higher initiation rates also has negative effects. In addition to the need for stronger, more expensive light sources, higher light intensities increase the population of primary radicals (radicals derived directly from photocleavage of the initiator). Large primary radical populations can lead to a phenomenon known as primary radical termination, which can reduce the polymerization rate.

To control photopolymerizations properly, the aforementioned negative effects must be well understood. This work first develops a homogeneous kinetic model, including diffusion-controlled kinetics, that describes the polymerization behavior in an optically thin sample. For this study, the model system is the polymerization of 2-hydroxyethyl methacrylate (HEMA) initiated by 2,2-dimethoxy-2-phenylacetophenone (DMPA). The influence of incident light intensity and photoinitiator concentration are briefly examined. These model predictions are compared to experimental rate profiles generated here for the HEMA/DMPA system and previously published for similar methacrylate systems (*8*). At higher light intensities, the effect of primary radical termination can be examined through the use of the homogeneous model. It is seen that as primary radical termination increases, autoacceleration is decreased and then eliminated, and the classical square root dependence of polymerization rate on light intensity no longer holds. To relate these effects to commercial polymerizations, the homogeneous model is incorporated into a one dimensional, spatially varying kinetic model to account for decreases in light intensity as a function of depth. 1D model predictions are presented for both conventional initiators (such as DMPA) and photobleaching initiators.

Homogeneous Model Development

In order to model photopolymerizations properly, the basic reaction mechanisms must be known. For the HEMA/DMPA system, neglecting chain transfer and inhibition/retardation, the overall mechanism is:

Initiation:

$$I \xrightarrow{h\nu} 2R\bullet \quad \textbf{(1a)}$$

$$R\bullet + M \xrightarrow{k_i} P_1\bullet \quad \textbf{(1b)}$$

Propagation:

$$P_n\bullet + M \xrightarrow{k_p} P_{n+1}\bullet \quad \textbf{(1c)}$$

Termination:

$$P_n\bullet + P_m\bullet \xrightarrow{k_t} P_{n+m} \quad (P_n + P_m) \quad \textbf{(1d)}$$

$$P_n\bullet + R\bullet \xrightarrow{k_{tp}} P_nR \quad \textbf{(1e)}$$

In these equations, I represents the initiator species, M is monomer, P_n, P_m, and P_{n+m} are dead polymer chains, and P_nR is dead polymer produced via primary radical termination. R• and P_n• represent primary radicals and growing macroradical chains of n repeating units, respectively.

Initiation is broken into two steps: photocleavage of initiator molecules to produce primary radicals (equation 1a) and the initiation of growing polymer chains (equation 1b). k_i is the kinetic constant for the chain initiation step, and the rate of step 1a is given by:

$$R_i = 2\phi\varepsilon I_0 b[I] \quad \textbf{(2)}$$

where ϕ is the initiator efficiency, ε is the molar absorptivity of the initiator, I_0b is the incident light intensity in moles of photons per square centimeter per second and [I] is the instantaneous initiator concentration. The 2 represents the generation of two primary radicals for each initiator molecule; in this study the two primary radicals are assumed to have identical diffusive and reactive characteristics. The properties for DMPA used in the model are listed in Table I, where the value for the efficiency, 0.6, is a typical value for free radical initiators.

Table I. Material and Kinetic Properties for DMPA and HEMA

Initiator Properties for DMPA:		
ε = 150 L/mol·cm	ϕ = 0.6	
Material Properties for HEMA:		
ρ_m = 1.073 g/cm^3	ρ_p = 1.15 g/cm^3	$[M]_0$ = 8.2 mol/L
T_{gm} = -60 °C	T_{gp} = 55 °C	
α_m = 0.0005 °C^{-1}	α_p = 0.000075 °C^{-1}	
Kinetic Parameters for HEMA:		
R = 4 L/mol[a]		
k_{p0} = 1000 L/mol·s	A_p = 0.66	f_{cp} = 0.042
k_{t0} = 1.1 x 10^6 L/mol·s	A_t = 1.2	f_{ct} = 0.060
k_{i0} = 1000 L/mol·s	A_i = 0.66	f_{ci} = 0.042
k_{tp0} = varies	A_{tp} = 0.66	f_{ctp} = 0.042

[a]The reaction-diffusion parameter, R, is from C. N. Bowman (unpublished data).

In the propagation step (equation 1c), monomer is added to the growing polymer chains with kinetic constant k_p. All growing polymer chains ($n \geq 1$) are assumed to be identical, *i.e.*, they have the same reactivities. Termination can occur through two mechanisms. Bimolecular termination (equation 1d) can occur through either combination or disproportionation. Since the mode of bimolecular termination does not influence the kinetics, a single termination kinetic constant (k_t) accounting for both modes will be used. In primary radical termination (equation 1e), a growing polymer chain is terminated by reacting with a primary radical produced from initiator photocleavage. The primary radical termination kinetic constant (k_{tp}) will in general be different from k_t, due to the difference in reactivity and diffusivity between macroradicals and primary radicals.

Once the general mechanism is known, the model development is straightforward. Species balances are performed for the six reacting species in the system: initiator, primary radicals, monomer, growing macroradicals, dead polymer, and primary radical-terminated polymer. An example of such a species balance for the growing macroradicals is:

$$\frac{d[P_n \bullet]}{dt} = k_i[R\bullet][M] - 2k_t[P_n \bullet]^2 - k_{tp}[R\bullet][P_n \bullet] \quad (3)$$

The six species balances, coupled with kinetic constant expressions and correlations between conversion and fractional free volume, are integrated numerically to provided concentration profiles. From these data, rate-conversion-time relations can be developed.

The expressions for the kinetic constants used in this work are those derived for diffusion-controlled kinetics (*9-11*). Following the work of Anseth and Bowman (*12*) the expressions for the propagation and termination kinetic constants are:

$$k_p = \frac{k_{p0}}{\left(1 + e^{A_p\left(1/f - 1/f_{cp}\right)}\right)} \quad (4a)$$

$$k_t = \frac{k_{t0}}{\left(1 + \left(\frac{Rk_p[M]}{k_{t0}} + e^{-A_t\left(1/f - 1/f_{ct}\right)}\right)^{-1}\right)} \quad (4b)$$

In the expression for k_p, k_{p0} is the true kinetic constant for propagation in the absence of all diffusional limitations, A_p is a parameter governing the rate of decrease of k_p in the diffusion-controlled regime, f is the fractional free volume of the polymerizing system and f_{cp} is the critical fractional free volume for propagation, *i.e.*, the fractional free volume value at which k_p is half k_{p0}. The forms for k_i and k_{tp} are assumed to be identical to equation 4a, with similar parameters governing their diffusional dependence. The expression for k_t has an extra term to account for reaction diffusion. In that term, R is the reaction diffusion parameter and [M] is the instantaneous monomer concentration (or, more correctly, unreacted double bond concentration, in the case of multifunctional monomers).

A method for determining the kinetic parameters for propagation and bimolecular termination has previously been presented (*13*). The technique requires a single experimental rate versus conversion profile and will not be reiterated here. The values determined for HEMA in that work will be used for this work and are found in Table I. Finding values for the parameters governing chain initiation and primary radical termination is not as straightforward. In this work, two assumptions will be made. First, since chain initiation and primary radical termination both rely on the diffusion of small molecules (R• and M for chain initiation and R• for primary radical termination), their diffusional characteristics will be assumed to be identical to propagation. Thus $A_{tp} = A_i = A_p$ and $f_{ctp} = f_{ci} = f_{cp}$. Second, k_{i0} will be approximated by k_{p0}, since it is essentially a radical propagation reaction. k_{tp0} will not be fixed. In fact, its value will be varied in the simulations to determine the relative effect of primary radical termination on the polymerization rate profile.

Experimental

For the experiments, HEMA was obtained from Aldrich (Milwaukee, WI) and was dehibited prior to use. DMPA was obtained from Ciba-Geigy (Hawthorne, NY) and used as received. The polymerizations were performed in a Perkin-Elmer differential scanning calorimeter (DSC) equipped with a photoaccessory. The photoaccessory includes a monochromator, and 365 nm ultraviolet light was used to initiate the polymerizations. A light intensity of 3.8 mW/cm^2 was used for the polymerizations. The polymerization rate is determined by monitoring the rate of heat evolution and normalizing by the standard heat of reaction for methacrylates, -13.1 kcal/mol (*14*). Samples were limited to 2 to 3 milligrams to ensure the validity of the thin film approximation for light absorption. A nitrogen purge was used prior to and during the DSC runs to prevent oxygen inhibition of the free radical polymerizations.

Results and Discussion

Homogeneous Kinetic Model. The validity of the homogeneous model for predicting rate profiles at low light intensities and a single low initiator concentration has already been established (*15*). When the initial initiator concentration is increased, the polymerization rate increases accordingly, as shown in Figure 1. The simulation predicts the rate profiles rather well, giving good agreement in the absence of diffusional limitations, throughout the autoacceleration and autodeceleration regimes, up to the final limiting conversion. The simulation shows the classical square root dependence of polymerization rate on initiation rate in the absence of primary radical termination. As the light intensity is held constant, the rate of initiation is proportional to the initiator concentration (equation 2). Thus, the rate profiles scale with the square root of the initiator concentration. This scaling effect has also been previously reported for HEMA polymerizations initiated thermally by 2,2'-azobis(isobutyronitrile) (*8*).

The rate of initiation can also be changed by varying the incident light intensity while the initiator concentration is held constant. Homogeneous model predictions for a three order of magnitude range of light intensities at a fixed initiator concentration are shown in Figure 2. Once again, the square root dependence of polymerization rate on initiation rate is seen. The reason for this dependence becomes clear when the species balance for the macroradical concentration (equation 3) is examined. After the initial macroradical population is established, the pseudo-steady state assumption can be applied to equation 3. In the absence of primary radical termination, chain initiation must balance bimolecular termination. Equating the first and second terms on the right hand side of equation 3, it is seen that the macroradical concentration varies with the square root of the primary radical concentration, and thus, initiation rate.

When primary radical termination becomes the dominant mechanism of termination, the square root dependence is no longer seen, as witnessed in Figure 3. At

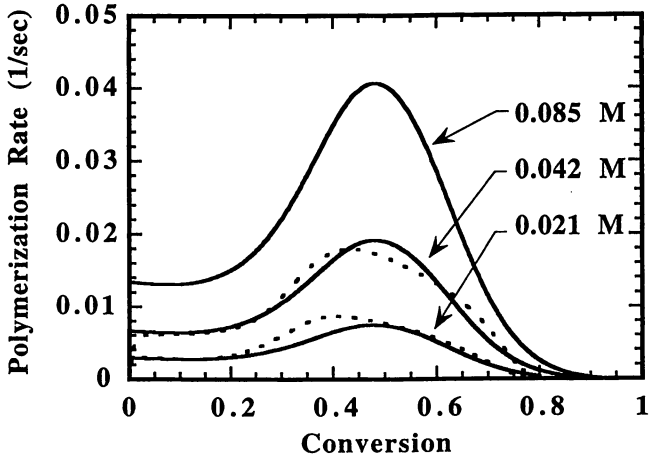

Figure 1. Experimental polymerization rate profiles (dotted lines) compared to model predictions (solid lines) for several different initial initiator concentrations. Primary radical termination effects are not included in the simulation ($k_{tp0} = 0$).

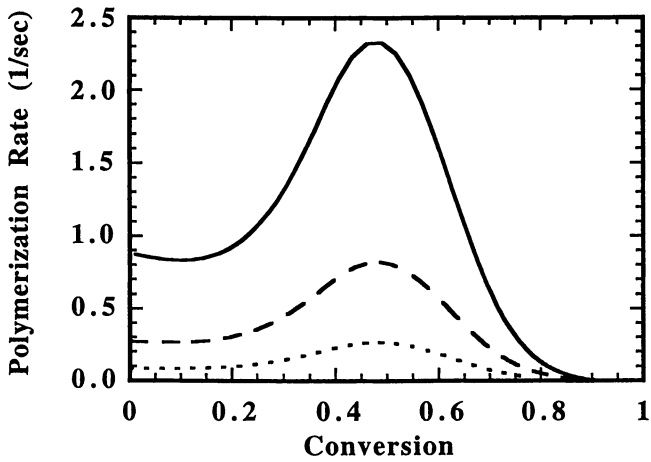

Figure 2. Polymerization rate as a function of incident light intensity as predicted by the homogeneous kinetic model. The lines correspond to 100 mW/cm^2 (solid), 10 mW/cm^2 (dashed) and 1 mW/cm^2 (dotted). The initiator is 0.021 M (0.5 weight percent) DMPA; primary radical termination is not included ($k_{tp0} = 0$).

lower light intensities (the 1 mW/cm^2 curve), the balance between chain initiation and bimolecular termination still dictates the macroradical concentration, and the square root dependence still holds. The rate curve resembles the profiles seen previously in Figure 2. As the light intensity is increased to 10 mW/cm^2, primary radical termination effects become apparent. At lower conversions, the rate still scales with light intensity. Once autoacceleration begins, however, the correlation breaks down. The scaled polymerization rate is below the value predicted by the pseudo-steady state analysis of equation 3. As the light intensity is increased, the reduction in rate becomes greater and manifests earlier. At the highest light intensity (1000 mW/cm^2), the rate is greatly depressed, to the point of autoacceleration being nearly eliminated.

The reason behind this phenomenon is as follows: at low light intensities, the primary radical population is relatively low. In equation 3, bimolecular termination (the second term) dominates primary radical termination (the third term). The balance determining the macroradical population is still between chain initiation and bimolecular termination. At high light intensities (high primary radical concentrations), primary radical termination is the dominant mechanism of termination and balances chain initiation. Setting the first and third terms equal on the right hand side of equation 3 causes the primary radical concentrations to cancel, and the macroradical concentration becomes independent of primary radical concentration and therefore light intensity. Not only is the macroradical concentration now independent of light intensity, but it is also reduced due to the quenching effect of the primary radicals.

At intermediate light intensities (such as 10 or 100 mW/cm^2), bimolecular termination dominates at lower conversions, but as k_t starts to decrease in the autoacceleration region, bimolecular termination drops while primary radical termination remains constant. Thus, the balance shifts from bimolecular to primary radical termination. Primary radicals now quench the build-up of macroradicals, leading to large reductions in the height of the autoacceleration peak. Further, more detailed studies on the effects of primary radical termination on polymerization rate are reported in Goodner and Bowman (*16*).

Kinetic Model with Spatial Variations. While the previous examinations give insight into the polymerization behavior response as light intensity and initiator concentration are changed, they reflect the polymerization in an optically thin film. In real processes, however, the light intensity can decrease markedly with depth into a film, especially at low light intensities and high initiator or pigment concentrations (*17*). In order to treat the polymerization kinetics properly in these optically thick films, a slightly different approach must be taken. The simplest route is to divide the thick sample into many optically thin slices, over which the light intensity does not change appreciably due to absorbance by chromophores such as initiator molecules. The homogeneous kinetic model can then be applied to each slice at a given time step, and the light intensity profile across all slices can be recomputed between time steps (by applying Beer's law). This scheme is reflected in Figure 4; the resulting model incorporating spatial variations will hereafter be referred to as the '1D Model'. For the preliminary results of the 1D model reported here, the simplifying assumptions of no mass and heat transfer across the slices are made. Additionally, the sample is assumed to be isothermal, *i.e.*, all slices are at the same temperature and the temperature does not change as the reaction proceeds. While these assumptions will be invalid for either high polymerization rates or high double bond conversions, they provide a good first approximation and give insight into the general trends in the polymerization behavior.

The rate profile predicted by the 1D model for low light intensity and initiator concentration is shown in Figure 5. It is apparent that the thin-film approximation for light intensity still holds across a 3 mm thick film for these low values. The rate profiles at the top and bottom of the film are nearly identical. A slight delay - approximately 20 seconds - is seen for both the onset of autoacceleration and the time for maximum rate (which occurs around 170 seconds at the top of the sample); this

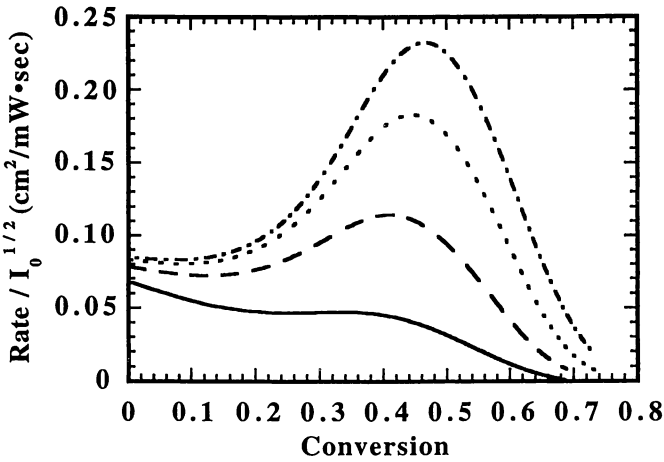

Figure 3. Scaled polymerization rate as a function of incident light intensity as predicted by the homogeneous kinetic model. The lines correspond to 1000 mW/cm^2 (solid), 100 mW/cm^2 (dashed), 10 mW/cm^2 (dotted) and 1 mW/cm^2 (dash-dot). The initiator is 0.021 M (0.5 weight percent) DMPA; primary radical termination is included (k_{tp0} = 1.0 x 10^7).

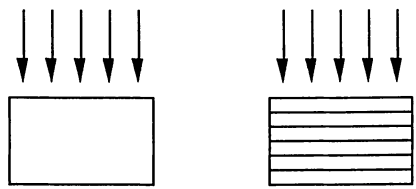

Figure 4. Comparison of the homogeneous kinetic model to the 1D model. Arrows indicate the direction of light illumination.

feature is caused by the slightly reduced light intensity at the bottom of the film. From a processing point of view, though, the variations are slight enough to treat the sample as uniform, and reaching the specified conversion at the top of the film would be sufficient to satisfy product specifications.

If the initiator concentration is increased to 0.05 M (corresponding to a little over 1 weight percent), the heterogeneity seen throughout the sample is quite pronounced. Figure 6a shows the rate profile with respect to time and depth into the sample. At the top of the film, a normal profile is seen, with no diffusion-controlled kinetics up to 20 seconds, followed by autoacceleration and autodeceleration down to a small, near zero, rate. The polymerization behavior at the bottom of the film shows a similar profile, but with a marked decrease in rate and greatly delayed onset of autoacceleration. The maximum rate is not reached at the bottom of the film until 100 seconds, and the maximum rate that is achieved is less than a quarter of the value seen at the top of the film.

Another way to examine the influence of optical thickness resides in the conversion versus time and depth data shown in Figure 6b. After polymerizing for 75 seconds, 75 percent of the monomer in the system is incorporated into polymer chains at the top of the film. In contrast, the bottom of the film shows less than 30 percent conversion, leaving a great deal of monomer unincorporated and leachable, devastating the mechanical properties of the film and raising serious toxicity concerns. Remedying this problem requires considerable effort. For example, if a conversion of 60 percent is needed to reach product specifications, this condition is met after 50 seconds at the top of the film. However, because of the attenuated light intensity, sixty percent conversion is not reached until after 150 seconds at three millimeters depth, causing a three-fold increase in processing time.

Increasing the initiator content further would merely serve to increase the optical density of the sample, limiting light penetration and exaggerating the problems seen in the previous figures. If higher initiator concentrations are needed, one possible solution to the problem is the use of a photobleaching initiator. Upon cleavage, a photobleaching initiator loses some or all of its absorptivity at the illuminating wavelength.

Model predictions using 0.5 M photobleaching initiator are shown in Figure 7. In this set of data, the initiator has the same efficiency and molar absorptivity at 365 nm, but is assumed to lose all absorptivity at 365 nm after photocleavage. Initially, a high rate of polymerization is reached in a small region near the top of the film into which the light can effectively penetrate. After polymerization in this region, the polymerization proceeds along a polymerization front. The front propagates into the film as the excess initiator in the polymerized region cleaves and becomes transparent. While the polymerization proceeds at relatively slow rates compared to the lower initiator concentrations where the thin-film approximation holds, the use of a photobleaching initiator allows higher concentrations to be used to give higher initiation rates.

Conclusions

In this paper, the effect of incident light intensity and photoinitiator concentration on the radical photopolymerization of HEMA initiated by DMPA has been studied using both homogeneous and spatially varying kinetic models. These models are based on numerically integrating species balances of the reacting species in the system. Additionally, experimental studies have been performed to verify the accuracy of the homogeneous kinetic model predictions.

From the homogeneous model predictions, the effect of primary radical termination can be seen (as shown in Figure 3). At high light intensities and high initiator concentrations, primary radical termination reduces the increase in polymerization rate afforded by autoacceleration and decreases the final conversion.

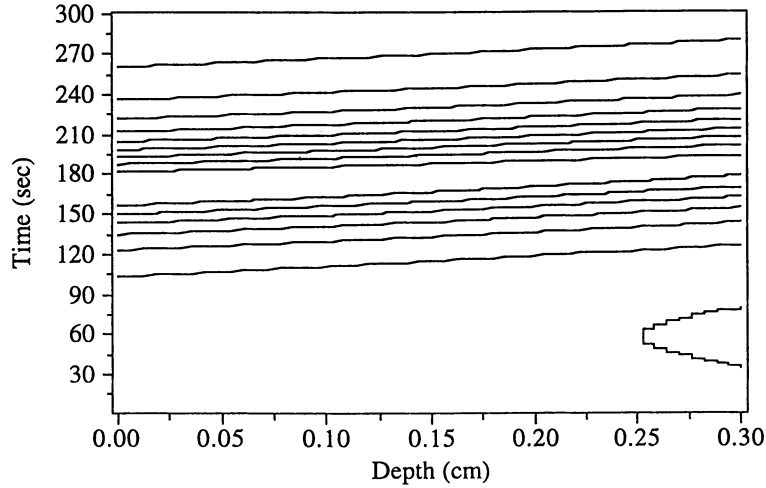

Figure 5. Rate versus time and depth as predicted by the 1D model for the polymerization of HEMA in a 3 mm thick film. Contours are spaced every 0.004 sec^{-1}. $[I]_0$ = 0.005 M DMPA and I_0 = 4.0 mW/cm^2.

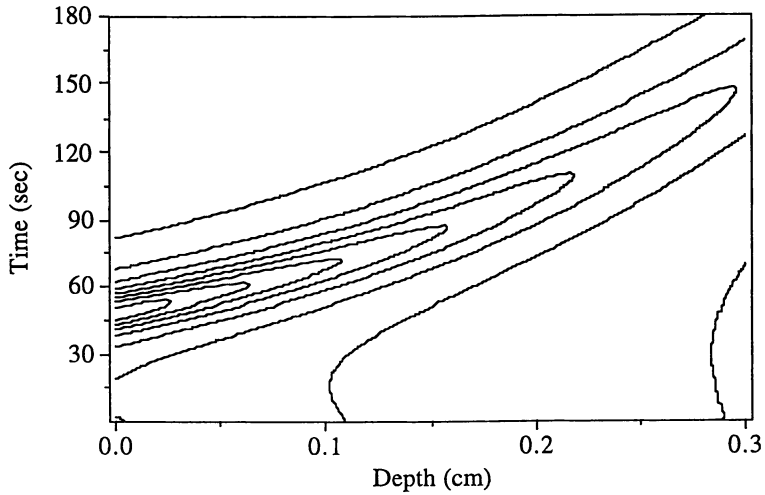

Figure 6a. Rate versus time and depth as predicted by the 1D model for the polymerization of HEMA in a 3 mm thick film. Contours are spaced every 0.02 sec^{-1}. $[I]_0$ = 0.05 M DMPA and I_0 = 4.0 mW/cm^2.

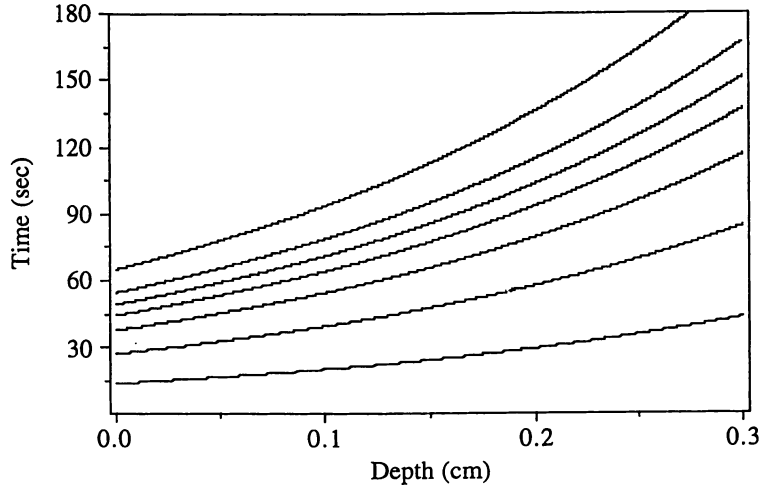

Figure 6b. Conversion versus time and depth for the polymerization shown in Figure 6a. Contours are spaced every 10 percent conversion.

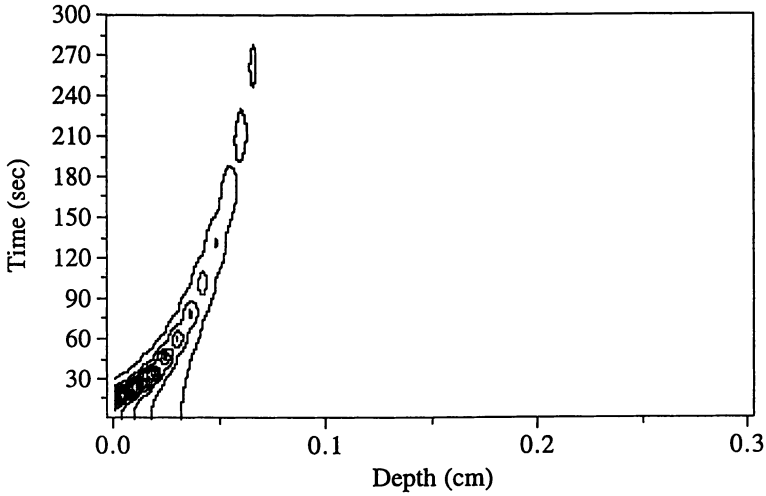

Figure 7. Rate versus time and depth as predicted by the 1D model for the polymerization of HEMA in a 3 mm thick film. Contours are spaced every 0.04 sec^{-1}. $[I]_0$ = 0.5 M photobleaching initiator and I_0 = 4.0 mW/cm^2. The beaded appearance along the polymerization front is a phenomenon of interpolation to the grid by the presentation software; it does not represent any physical phenomenon.

The effects of sample thickness are shown by the 1D model results. As initiator concentration is increased, light absorption throughout the film decreases the light intensity and, hence, the rate of polymerization at the bottom of the film. This decreased rate results in lower conversions and increased processing times, which must be accounted for in the production of commercially viable products. While not completely eliminating the problem, the use of photobleaching initiators mitigates the effects of high optical densities.

Acknowledgments

The authors would like to acknowledge the National Science Foundation for its support of this work through the Presidential Faculty Fellowship to CNB (CTS-9453369) and a graduate fellowship to MDG as well as 3M and the Camille Dreyfus Teacher-Scholar program.

Literature Cited

1. Kloosterboer, J. G. *Adv. Polym. Sci.* **1988**, *84*, 1-61.
2. Kannurpatti, A. R.; Peiffer, R. W.; Guymon, C. A.; Bowman, C. N. in *Critical Reviews of Optical Science and Technology: Polymers in Optics: Physics, Chemistry, and Applications*; Lessard, R. A. and Frank, W. F., Ed., **1996**; Vol. CR63, pp 136.
3. Decker, C. *Prog. Polym. Sci.* **1996**, *21*, 593-650.
4. Anseth, K. S.; Newman, S. M.; Bowman, C. N. *Adv. Polym. Sci.* **1995**, *122*, 177-217.
5. Bowman, C. N.; Peppas, N. A. *Macromolecules* **1991**, *24*, 1914-1920.
6. Anseth, K. S.; Bowman, C. N.; Peppas, N. A. *J. Polym. Sci. Polym. Chem.* **1994**, *32*, 139-147.
7. Kloosterboer, J. G.; Lijten, G. F. C. M. in *Cross-Linked Polymers: Chemistry, Properties, and Applications*; Dickie, R. A., Labana, S. S. and Bauer, R. S., Ed.; American Chemical Society: Washington, D.C., **1988**; Vol. 367, pp 409-426.
8. Scranton, A. B.; Bowman, C. N.; Klier, J.; Peppas, N. A. *Polymer* **1992**, *33*, 1683-1689.
9. Marten, F. L.; Hamielec, A. E. *J. Appl. Polym. Sci.* **1982**, *27*, 489-505.
10. Marten, F.; Hamielec, A. in *Polymerization Reactors and Processes*; Henderson, J. and Bouton, T., Ed.; American Chemical Society: Washington D. C., **1978**; Vol. 104, pp 43-69.
11. Soh, S. K.; Sundberg, D. C. *J. Polym. Sci. Polym. Chem.* **1982**, *20*, 1299-1313.
12. Anseth, K. S.; Bowman, C. N. *Polym. React. Eng.* **1993**, *1*, 499-520.
13. Goodner, M. D.; Lee, H. R.; Bowman, C. N. *Ind. Eng. Chem. Res.* **1997**, *36*, 1247-1252.
14. Cook, W. D. *Polymer* **1992**, *33*, 2152-2161.
15. Kannurpatti, A. R.; Goodner, M. D.; Lee, H. R.; Bowman, C. N. in ; Scranton, A. B., Ed.; American Chemical Society: Washington, D.C., **1997**.
16. Goodner, M. D.; Bowman, C. N. *Polym. React. Eng.* **in preparation.**
17. Cook, W. D. *J. Appl. Polym. Sci.* **1991**, *42*, 2209-2222.